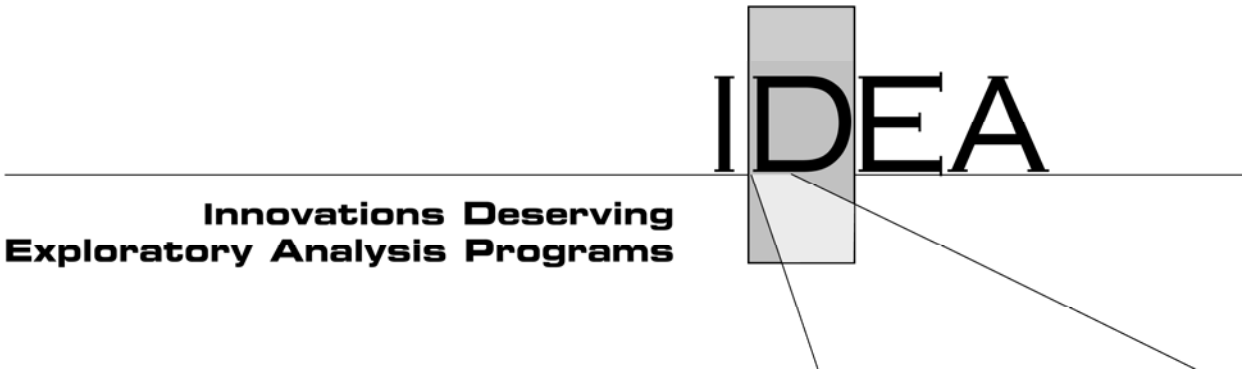

High-Speed Rail IDEA Program

DEVELOPMENT OF A COMMERCIAL-GRADE BI-AXIAL STRAIN TRANSDUCER

Final Report for High-Speed Rail IDEA Project 28

Prepared by:
Hosin "David" Lee, Principal Investigator
Public Policy Center
University of Iowa

September 2004

TRANSPORTATION RESEARCH BOARD
OF THE NATIONAL ACADEMIES

INNOVATIONS DESERVING EXPLORATORY ANALYSIS (IDEA) PROGRAMS MANAGED BY THE TRANSPORTATION RESEARCH BOARD

This investigation was performed as part of the High-Speed Rail IDEA program supports innovative methods and technology in support of the Federal Railroad Administration's (FRA) next-generation high-speed rail technology development program.

The High-Speed Rail IDEA program is one of four IDEA programs managed by TRB. The other IDEA programs are listed below.

- NCHRP Highway IDEA focuses on advances in the design, construction, safety, and maintenance of highway systems, is part of the National Cooperative Highway Research Program.
- Transit IDEA focuses on development and testing of innovative concepts and methods for improving transit practice. The Transit IDEA Program is part of the Transit Cooperative Research Program, a cooperative effort of the Federal Transit Administration (FTA), the Transportation Research Board (TRB) and the Transit Development Corporation, a nonprofit educational and research organization of the American Public Transportation Association. The program is funded by the FTA and is managed by TRB.
- Safety IDEA focuses on innovative approaches to improving motor carrier, railroad, and highway safety. The program is supported by the Federal Motor Carrier Safety Administration and the FRA.

Management of the four IDEA programs is integrated to promote the development and testing of nontraditional and innovative concepts, methods, and technologies for surface transportation.

For information on the IDEA programs, contact the IDEA programs office by telephone (202-334-3310); by fax (202-334-3471); or on the Internet at http://www.trb.org/idea

IDEA Programs
Transportation Research Board
500 Fifth Street, NW
Washington, DC 20001

DEVELOPMENT OF A COMMERCIAL-GRADE BI-AXIAL STRAIN TRANSDUCER

IDEA Program Final Report
For the Period 4/2002 through 2/2004
HSR-28

Prepared for
The IDEA Program
Transportation Research Board
National Research Council

Hosin "David" Lee, Principal Investigator
Public Policy Center
University of Iowa

September 12, 2004

TABLE OF CONTENTS

ABSTRACT

One of the most difficult parts of fatigue life estimation is obtaining accurate strain history data. Smart sensors and micro-electromechanical systems (MEMS) offer the potential of accurately monitoring the structural capacity of the rail infrastructure. The primary goal of this research was to develop a prototype MEMS-based intelligent Bi-Axial Strain Transducer (BiAST) and to assess its potential for monitoring and predicting the fatigue life of rail. The BiAST simultaneously measures strains in two perpendicular directions. Preliminary field testing of the BiASTs was conducted at the Transportation Technology Center, Inc. (TTCI) in Pueblo, Colorado to evaluate their performance and ruggedness. These field tests identified several problems that must be resolved before this technology can be successfully implemented. It was very difficult to install the BiAST sensors on the rail in the field. After installation, three of the five sensors didn't work at all, and the other two performed inconsistently. The current BiAST system lacked repeatability and accuracy. Attempts to incorporate a fatigue analysis module in the sensor system were unsuccessful. Any further development of this technology for such rail applications will require investigation of the causes of, and solutions to, the problems identified in this project.

KEYWORDS

micro-electro-mechanical system, fatigue analysis, strain gauge, Bi-Axial Strain Transducer, load cycle counting algorithm, peripheral interface controller, rail fatigue life.

EXECUTIVE SUMMARY

One of the most difficult parts of fatigue life estimation is obtaining accurate strain history data. A traditional, electric resistance strain gauge is inadequate for a long-term field test because of its relatively high non-linearity, drifting over time, self-heat effect, and lack of durability under harsh outdoor environments. The limited resources available for maintaining railroad infrastructure make it compulsory that we explore more effective ways of scrutinizing the health of that infrastructure. Smart sensors and micro-electromechanical systems (MEMS) are rapidly becoming a mainstream technology, and offer the potential of accurately monitoring the structural capacity of the rail infrastructure. The primary goal of this research was to develop a prototype MEMS-based intelligent Bi-Axial Strain Transducer (BiAST) and to assess its potential for monitoring and predicting the fatigue life of rail. The BiAST offers the potential for high resolution, a high sampling rate, absolute encoding, no strain drifting over time, and less measurement noise than analog-based strain sensors.

Under a previous High Speed Rail IDEA contract (HSR-15), we evaluated a prototype Uni-Axial Strain Transducer (UAST), a field-based micro-electro mechanical system (MEMS)/VLSI sensor that detects the movement of a patterned quartz emitter suspended above the surface of a VLSI IC chip containing an array of 64 detectors. Emitter movement is caused by surface strain in the structure being measured, where each of the detectors is coupled to AC-driven emitter fingers and generates voltage. The magnitude of strain can be determined from the phase of the sinusoidal waveform of the detector output. The maximum achievable strain can be calculated as ± 5,760 micro-strains with a resolution of 0.35 micro-strains (2.5 nm).

This project involved the evaluation of a more advanced prototype Bi-Axial Strain Transducer (BiAST) to simultaneously measure strains in two perpendicular directions. The BiASTs have a 15-bit output (from 0 to 32,767 counts), which represents a dynamic range of 224 microns. Using a 0.50-inch gage length (12.7 mm), the dynamic range for the sensors is thus 17,600 micro-strains, with one count of output representing 0.54 micro-strains. The design also included detachable mounting stems to facilitate installation, calibration, and removal from the rail.

To monitor the cyclic loading of the railroad track, Sarcos Research, a subcontractor of the University of Iowa, provided five prototype BiAST's and a sensor network controller that interfaced with a PC. Figure EX-1 shows the BiAST strain sensors with the mechanical flexure and attachment clevis that clamp to mounting stems bonded to the rail surface. Preliminary field testing of the BiASTs was conducted to evaluate their accuracy and ruggedness. Since the BiAST was originally developed for application in the aerospace testing environment, it was necessary to evaluate it in a real-life rail infrastructure environment. We installed five networked BiASTs on a railroad track in the testing facilities at the Transportation Technology Center, Inc. (TTCI) in Pueblo, Colorado. The instrumented track was then subjected static loads using TTCI's Track Loading Vehicle (TLV) and then to known moving wheel loads from a test train.

Using the BiASTs, real-time strain data were collected continuously for several days. Each train lap was extracted from the raw data to monitor the real-time strain caused by a train passage. The field strain data identified the locations of the peaks and valleys caused by the bending and compression stresses of the running wheels. Maximum tensile strains were between 850 and 950 micro-strains, while maximum compressive strains were measured at around -300 micro-strains for all laps. During the field testing at TTCI, we experienced several problems with the prototype BiAST sensor system. These included difficulty in installing the sensors on the rail, failure of a controller box due to ambient weather conditions, and poor sensor performance. Three of the five sensors failed to work at all, and the other two were unstable and unreliable.

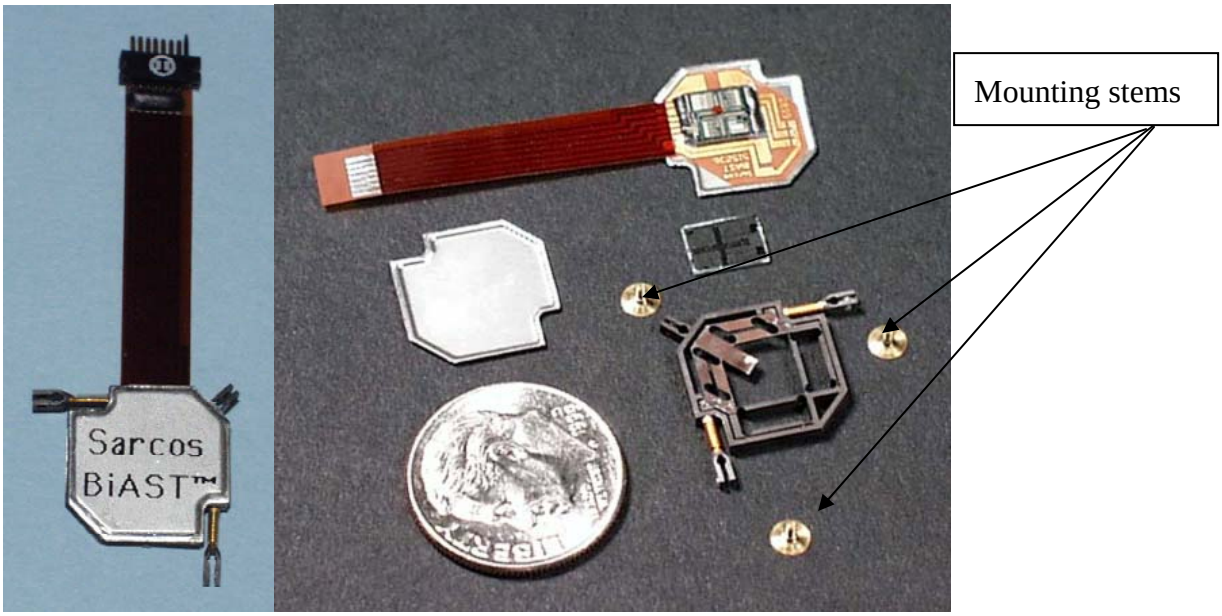

FIGURE EX-1 Prototype BiAST sensor and mounting stems.

A 3-D FEM model was developed to simulate a rail structure. The moving force model consisted of several load steps along the longitudinal direction of the rail. Each of the load steps was comprised of three orthogonal forces simulating the loads from one wheel passage in the transverse, vertical and longitudinal directions. Comprehensive real-time data from the field test were used to validate a rail fatigue model.

The final stage planned for this project was to correct the problems uncovered in the preliminary field tests and return to TTCI for final testing. The test section of rail was to be equipped with both BiAST sensors and conventional strain gage sensors to facilitate calibration and validation. Sarcos Research, however, was unable to provide the five self-powered load-cycle-counting controller boxes that were needed for the final field test. This was due to Sarcos' lack of success in completing the circuit board hardware with the Peripheral Interface Controller (PIC) microchip, and micro-controller software needed to implement a fatigue-modeling algorithm. As a result, we were not able to go back to TTCI for further testing. Although the hybrid BiAST incorporating the fatigue-modeling algorithm was not produced, the concept was demonstrated using a new PIC microcontroller.

In conclusion, this research identified significant problems with this concept that must be overcome if it is to be implemented. It was very difficult to install the BiAST sensors on the rail in the field. After installation, three of the five sensors didn't work at all, and the other two performed inconsistently. The BiAST system lacked repeatability and accuracy. Attempts to incorporate a fatigue analysis module in the sensor system were unsuccessful. Any further development of this technology for such rail applications will require investigation of the causes of, and solutions to, the problems identified in this project. .

1 INTRODUCTION

Heavier car loads and the resulting increases in axle loads have resulted in the need for improved management of rail fatigue life. One of the most critical failures of rail structure is caused by damage due to metal fatigue. Extensive railway fatigue literature exists on contact fatigue and crack propagation, but very few studies address crack initiation models (*1, 2; 3*). Lack of reliable in-field experimental data for fatigue-life prediction of railroad track is a critical issue in the fatigue design process (*4*). Design decisions based on laboratory testing cannot be taken for granted in the fatigue design process, where environment has a tremendous influence on the fatigue life of a component (*5*). Fatigue failure modes in rails are generally sudden, and if not promptly detected, can be catastrophic (6, 7; 8).

One of the most difficult parts of fatigue life estimation is obtaining accurate strain history data. A traditional, electric resistance strain gauge is inadequate for a long-term field test because of its relatively high non-linearity, drifting over time, self-heat effect, and lack of durability under harsh outdoor environments (*9*; *10*). The limited resources available for maintaining railroad infrastructure make it compulsory that we explore novel ways of scrutinizing the health of that infrastructure. Smart sensors and micro-electromechanical systems (MEMS) are rapidly becoming a mainstream technology, and offer the potential of accurately monitoring the structural capacity of the rail infrastructure *(11).* The primary goal of this research was to develop a prototype MEMS-based intelligent Bi-Axial Strain Transducer (BiAST) system and to assess its potential for monitoring and predicting the fatigue life of rail.

2 PROTOTYPE BI-AXIAL STRAIN TRANSDUCER SYSTEM

Under a previous High Speed Rail IDEA contract (HSR-15), a prototype uni-axial strain transducer (UAST™) package was developed with non-volatile RAM to store strain cycling history (*12*). The UAST is a MEMS that requires no calibration and features high resolution, variable sampling rates, absolute encoding, and low drift over time. The UAST was developed as a digital and absolute encoding device. It gives a maximum strain range of 11,500 με (± 5,750 με) and a resolution of 2.5 nm in displacement. Sampling rates can be configured with various strain resolutions. For instrumented structures where the load paths are unknown or constantly changing, however, a bi-axial strain sensor package was needed. Bi-axial strain measurements can be differenced to provide a high degree of temperature compensation and increased strain sensitivity. The BiAST was originally developed for strain measurement in the airframe of aging aircraft, which can take discrete airframe strain measurements and record the flight loads history.

The BiAST is a simple modification of the UAST. The BiAST consists of an emitter beam, a CMOS IC chip, connectors, sealed bi-axial mechanical flexure, and a sensor base assembly (*11*). The BiAST is an integrated MEMS with an analog-digital converter (A/D converter) and signal conditioning device inside of the package. It requires no additional measurement devices and is therefore highly portable. The BiAST measures small capacitive coupling signals generated between an array of electrostatic field emitters and an array of 64 field detectors on a CMOS IC chip. The BiAST has high resolution, a high sampling rate, and less signal noise than traditional strain gauges. The prototype BiAST device has a gage length of 12.7 mm and sits 2.34 mm above the rail surface. It utilizes a low-power UAST-QT chip and can measure strains in two perpendicular directions simultaneously. Figure 2-1 shows a fabricated prototype BiAST sensor, which was built using the parts and subassemblies shown on the right. Parts included an IC/sensor base assembly, a mechanical flexure assembly, an emitter, sensor cover, and the mounting stems.

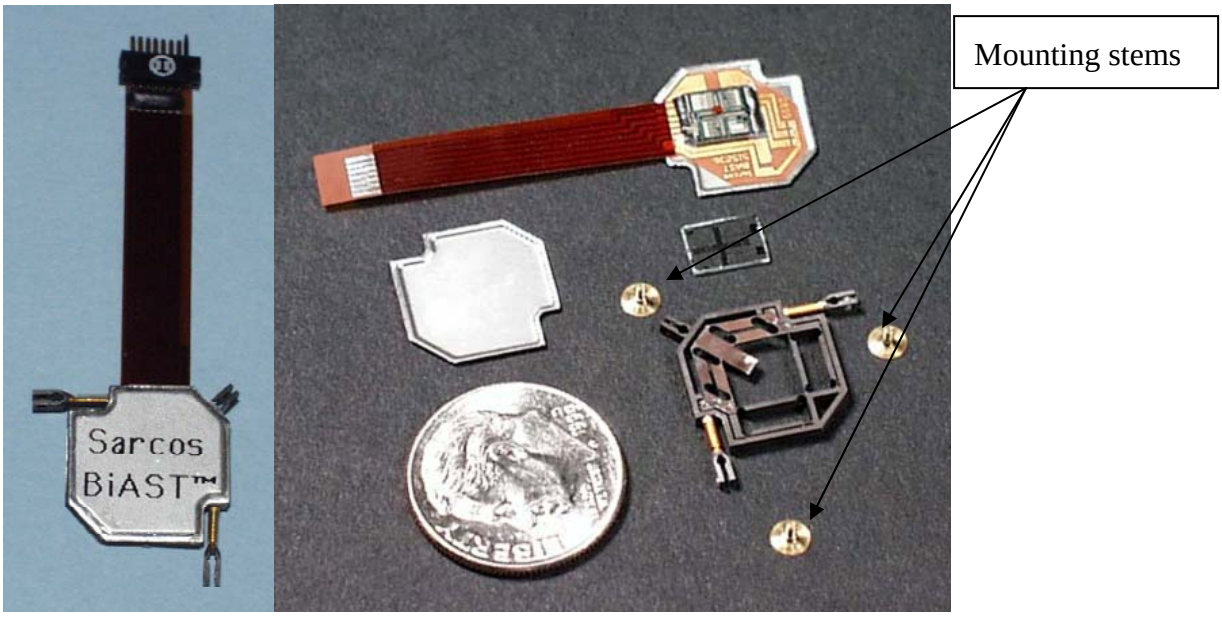

FIGURE 2-1 A fabricated prototype BiAST sensor and associated parts.
(Courtesy of Sarcos, Inc.)

2.1 THEORY OF OPERATION

As shown in Figure 2-2, the BiAST detects the movement of an emitter suspended above the surface of a CMOS IC chip containing an array of 64 charge-integrating field detectors. Emitter movement is caused by surface strain in the structure being measured. Each of the CMOS detectors is coupled to AC-driven emitter fingers, and generates voltage. The detector array and the emitter fingers are designed as a vernier, with a slight difference between the detector space and emitter finger space. The magnitude of strain can therefore be determined from the phase of sinusoidal waveform of the detector output. In order to calculate a strain value, the 64 analog detector values are first measured and converted to digital values. As shown in Figure 2-3.a, 32 of the 64 values should be inverted to form a single sinusoidal curve. The correlation function (Figure 2-3.c) is then computed by summing the products between each of the 64 digitized values and a series of 64 template values (Figure2-3.b). Finally, a binary search is performed to find a zero-axis crossing value of the correlation function, which indicates a computed strain value. Each emitter finger is spaced at 57.6 μm and the detector is at 55.8 μm. The maximum achievable strain and maximum resolution are ±5,760 micro-strains and 0.35 micro-strains, respectively.

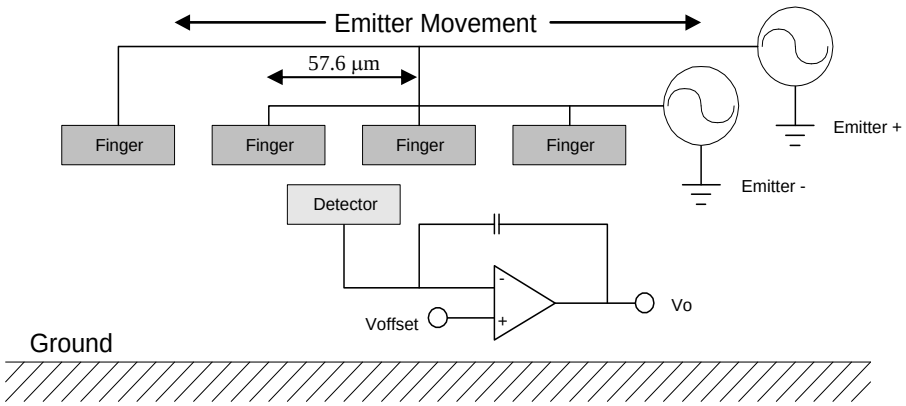

FIGURE 2-2 Emitter fingers and detector of BiAST (Courtesy of Sarcos Inc.).

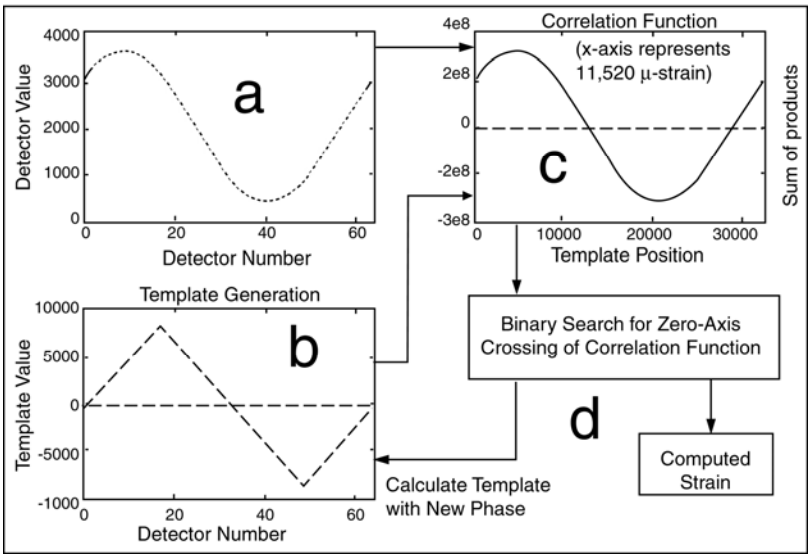

FIGURE 2-3 Operational theory of BiAST (Courtesy of Sarcos Inc.).

As shown in Figure 2-4, the BiAST system consists of three parts: a BiAST sensor, a networking controller box and a communication cable. The BiAST sensing chip has an on-chip decimation filter that allows a user to select how many samples the sensor should take and average before reporting the answer to the controller. Selectable decimation levels include 1x, 4x, 16x, and 128x, corresponding to sample rates of 1010, 505, 162 and 22 samples per second, respectively, for both axes. A typical RMS noise level for sensors using 1x decimation is about 4-8 counts (i.e., 1 count=0.45 με). Because the BiAST is battery operated, it is convenient for performing field tests at remote sites.

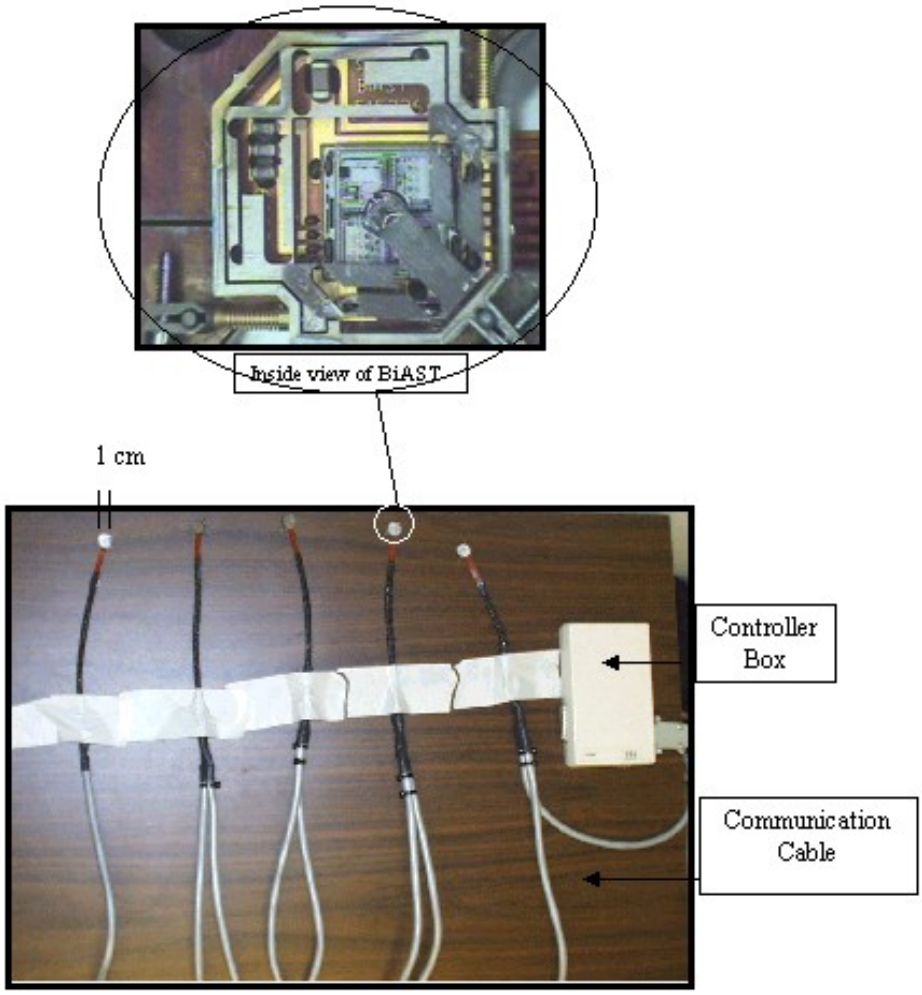

FIGURE 2-4 Five BiAST sensors connected to communication cables and controller box (13).

2.2 DATA ACQUISITION PROCEDURE

First, the BiAST sensors are plugged into the network cable. The controller box is configured to the desired decimation level using the configuration switches, and turned on to launch the data acquisition software. A user can print raw or statistical data to the screen or write data to a file. To change decimation levels, the user needs to reconfigure the switches and power-cycle of the network controller by resetting the switch. The software can process up to 3,000,000 raw samples at 1010 Hz (47 minutes without decimation). It also gives users the option of changing the maximum number of raw samples and the number of raw samples used in computing mean and standard deviation of strains.

Figures 2-5 and 2-6 show examples of 500 data points collected during laboratory tests from a rail without any load using two BiAST sensors, D and E, with a decimation level of 1 and at a data collection frequency of 1010 Hz. As can be seen from these figures, sensor D is more stable than the sensor E, where the strain data in the Y axis is skewed by 10 micro-strains with a few spurious points reaching to 30 micro-strains without loading.

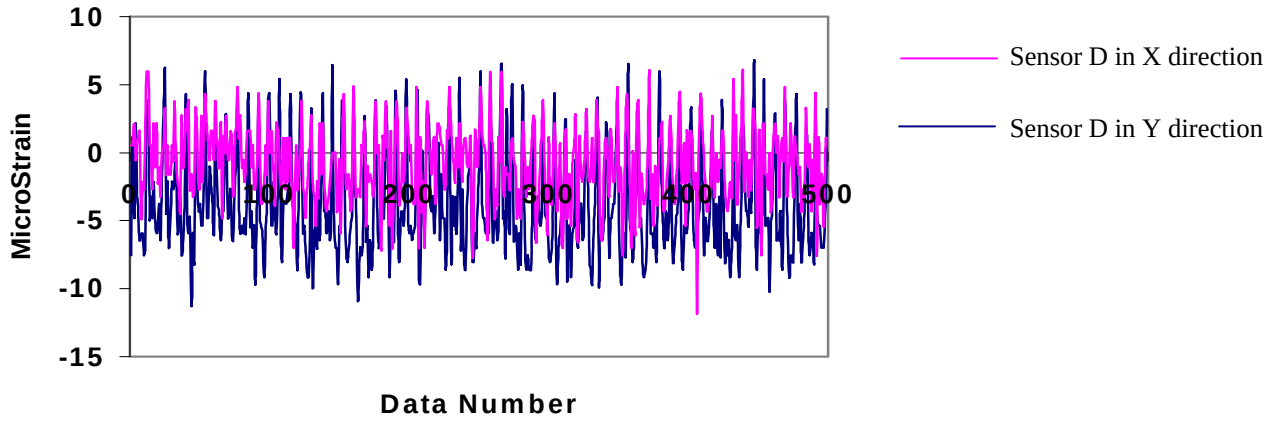

FIGURE 2-5 Noise collected from BiAST Sensor D.

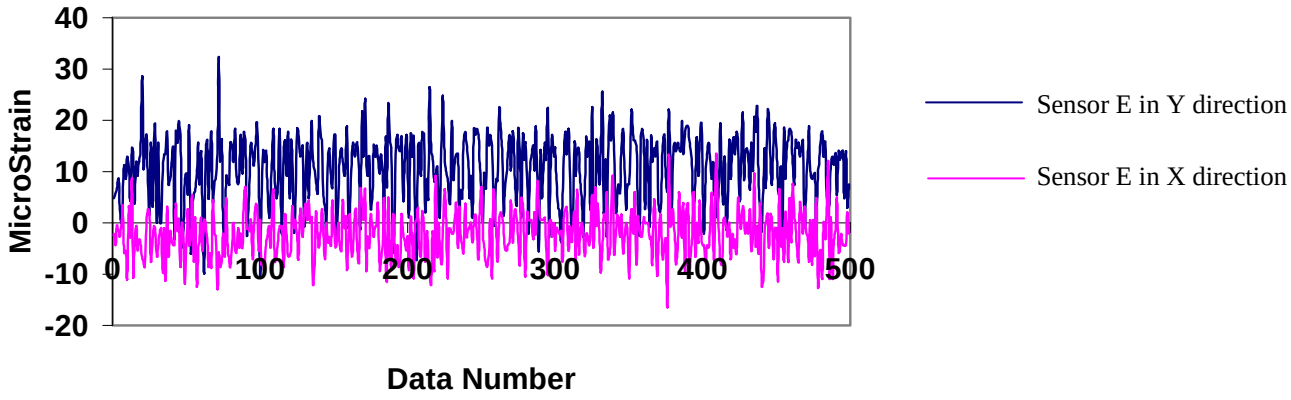

FIGURE 2-6 Noise collected from BiAST Sensor E.

A statistical analysis of strains was performed to determine the noise levels for BiAST's. The five BiAST's were tested for three times while being fixed on a flat surface. Five hundred raw data points were collected from each sensor. As summarized in Tables 2-1, sensors B, C, and D exhibited relatively small mean noise levels at around 5 micro-strains whereas sensors A and E exhibited significantly higher mean noise values. As shown in Table 2-2, the standard deviations of these measurements were around 5 micro-strains in B, C, and D sensors but significantly higher in the A and E sensors.

TABLE 2-1 Mean Values of 500 Data Points Collected from Five Sensors

No. of Trials	Axis	Average Noise (micro-strain)				
		D	E	B	C	A
1	Y-Axis	-5.83	-47.83	2.58	-1.18	14.23
	X-Axis	-1.44	13.41	-1.35	-2.59	-3.53
2	Y-Axis	-10.43	-91.56	5.29	-2.73	19.76
	X-Axis	4.01	27.05	-2.47	-8.51	-3.73
3	Y-Axis	-2.47	-33.32	1.69	-0.41	13.04
	X-Axis	5.92	-0.02	-1.91	-6.08	-1.74
Average	Y-Axis	-6.24	-57.57	3.19	-1.44	15.68
	X-Axis	2.83	13.48	-1.91	-5.72	-3.00

TABLE 2-2 Standard Deviation of 500 Data Points Collected from Five Sensors

No. of Trials	Axis	Standard Deviation of Noise (micro-strain)				
		D	E	B	C	A
1	Y-Axis	3.86	29.32	4.02	6.93	12.17
	X-Axis	2.74	11.98	1.68	4.43	2.41
2	Y-Axis	4.61	29.13	3.40	7.18	12.31
	X-Axis	3.03	5.49	1.60	4.55	2.13
3	Y-Axis	4.41	29.20	4.80	7.25	12.38
	X-Axis	3.55	12.09	1.65	2.64	2.22
Average S.D.	Y-Axis	4.29	29.22	4.08	7.12	12.29
	X-Axis	3.11	9.05	1.64	3.87	2.25

3 FINITE ELEMENT MODELING FOR RAIL STRUCTURES

To validate the BiAST-based fatigue life prediction, a finite element model was developed using ANSYS to compute strains within the rail structure and to locate critical locations. The developed FEM model is capable of simulating the complex loading configuration and geometry of rail structures. FEM is considered one of the most accurate methods for analyzing track (*14*; *15*), and is a vital step in the proposed methodology for evaluating the MEMS sensors to predict the fatigue life of rail at critical locations. The primary objective of the FEM model was to identify the critical locations, where BiAST were to be installed. Identifying the critical strain points is a very important task in investigating fatigue damage, which started by identifying the most crucial load step to cause highest stresses.

Both the rail and the cross tie were included in the FE analysis, as rail alone is not sufficient to model a rail system (*15*). As shown in Figure 3-1, the moving force model consists of load steps along the beam, each with three orthogonal forces, Px, Py, and Pz, simulating the loads from one wheel passage. A total span length was 17 inches between the centers of the cross ties and one half of the span was modeled with symmetrical boundary conditions on both ends of the track section. The bottom of the cross tie was fixed. The model was meshed with approximately 15,600 elements.

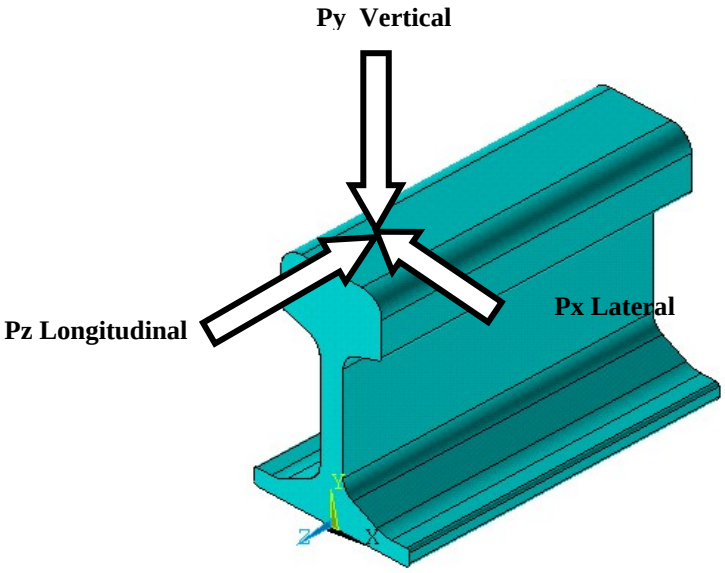

FIGURE 3-1 One load step consisting of three orthogonal forces of Px, Py and Pz.

The impact factor is the result of a combination of curving at speed, cross tie spacing, and moment of inertia of the rail. The angle is the result of the rail axis inclination, which causes the rail mounting slope on cross ties. The applied force for a 39,000 lb axle load can be calculated as follows (*14*).

Py = static wheel load * Cos (load angle) *impact factor at 40 mph = (39,000 lb) (Cos 2.862) (1.1) = 42,846 (lbs)

Pz corresponds to the transverse track forces that take the form of dynamic components. Dynamic force is caused by various forms of track defects and by rolling stock defects. Pz equal to approximately 5000 lbs was used and was calculated based on a semi-empirical equation (3.1).

$$Pz = \frac{AxleLoad * V(Km/h)}{1{,}000} \text{ , where V = train speed} \qquad (3.1)$$

Px corresponds to the frictional force caused by movement of the wheel on the rail. The coefficient of friction was assumed to be 0.2, and friction force to be equal to 5,800 lbs in the opposite direction for rolling (*16)*.

Based on this analysis, we identified five critical strain locations on the rail where the BiAST sensors should be installed (See Figure 4-5).

4 INSTALLATION AND STATIC LOAD TESTING

4.1 TEST SITE

The BiAST system was tested at the test track at Transportation Technology Center Inc. (TTCI) near Pueblo, Colorado. TTCI offers forty-eight miles of railroad track for different testing purposes. As shown in Figure 4-1, the 2.7-mile Facility for Accelerated Service Testing (FAST) loop is divided into many different test sections, including tangent sections, spiral sections, curved sections (three 5-degree and one 6-degree curve) and turnouts. In this study, Section 9 (tangent) and Section 25 (6-degree curve) were used to evaluate the BiAST. Test train operations are designed to accumulate up to 1.0 million gross tons a day at an operating speed of up to 40 miles per hour and heavy axle loads of 39 tons.

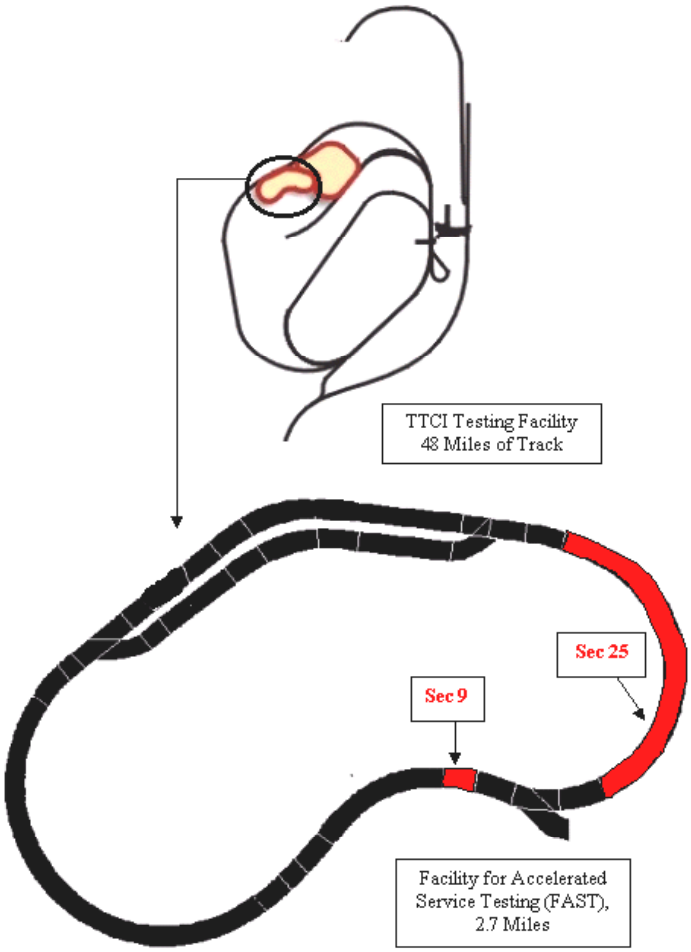

FIGURE 4-1. TTCI testing facility with FAST testing site with Sections 9 and 25 (Courtesy of TTCI).

4.2 INSTALLATION AND SYSTEM PREPARATION

For this study, the rail surface area was heated, ground, and cleaned to be ready for the adhesion of the mounting stems for the BiAST. Because the adhesives alone did not provide sufficient bond strength, the adhesive was used to hold the mounting stems on the rail before they were welded. The mounting stems were positioned using a tool that is custom made for the BiAST. Figure 4-2a shows this mounting tool and Figure 4-2b shows the attached stems. The BiAST's were then tightened to these stems with very small screws (see Figure 4-2c). The process of attaching the stems and tightening the BiAST's to them was extremely difficult as the bonded stems easily disengaged from the rail surface.

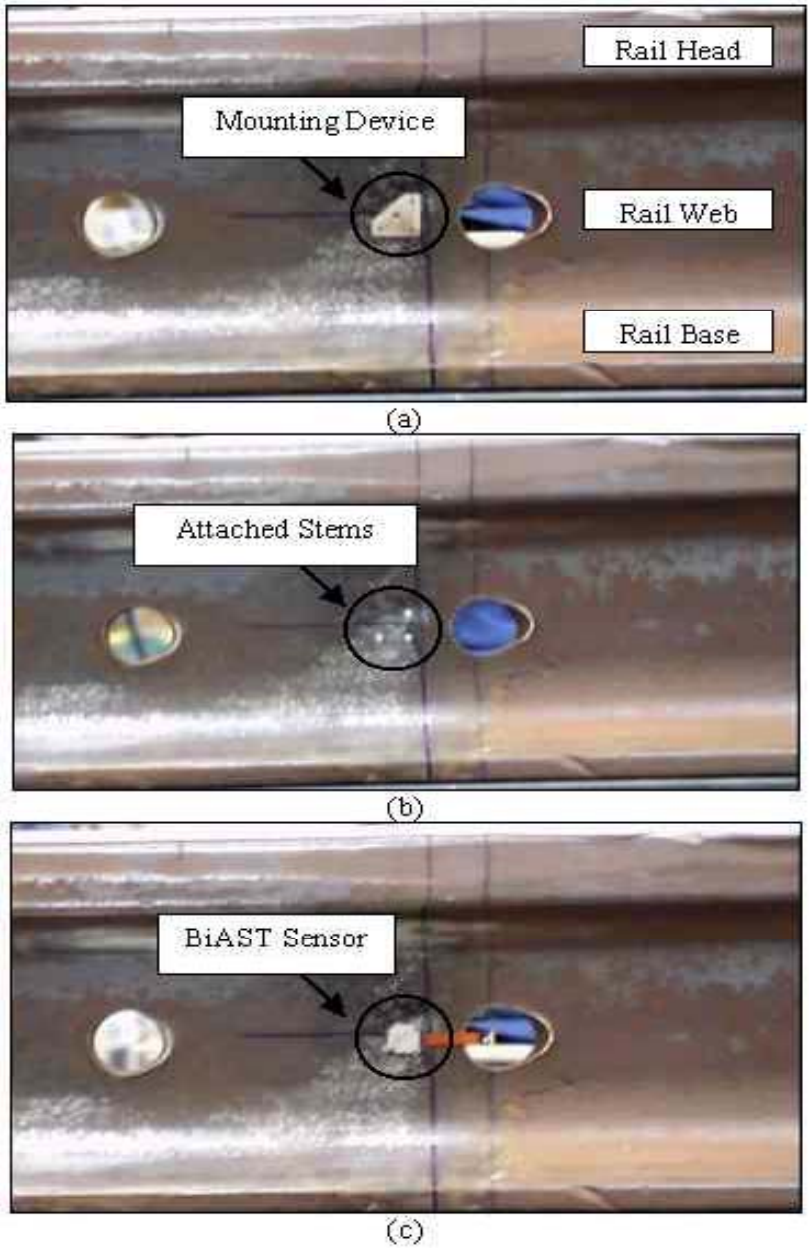

(a) Stem mounting tool, (b) Positioned stem (c) Tightening BiAST to the stems

Figure 4-2. Steps of installing and attaching BiAST system

The BiAST's were then connected to the controller box using a network cable. Due to the limited length of the flexible part of the cable, the rigid part of the cable had to be fixed to the rail using duct tape (see Figure 4-3). Mirrors had to be used to attach a BiAST at the bottom of the base. Given the limited length of the network cable, a van was parked near the test site to store all necessary equipment. The BiAST's were installed at the five critical locations that were identified by the 3-D FEM model.

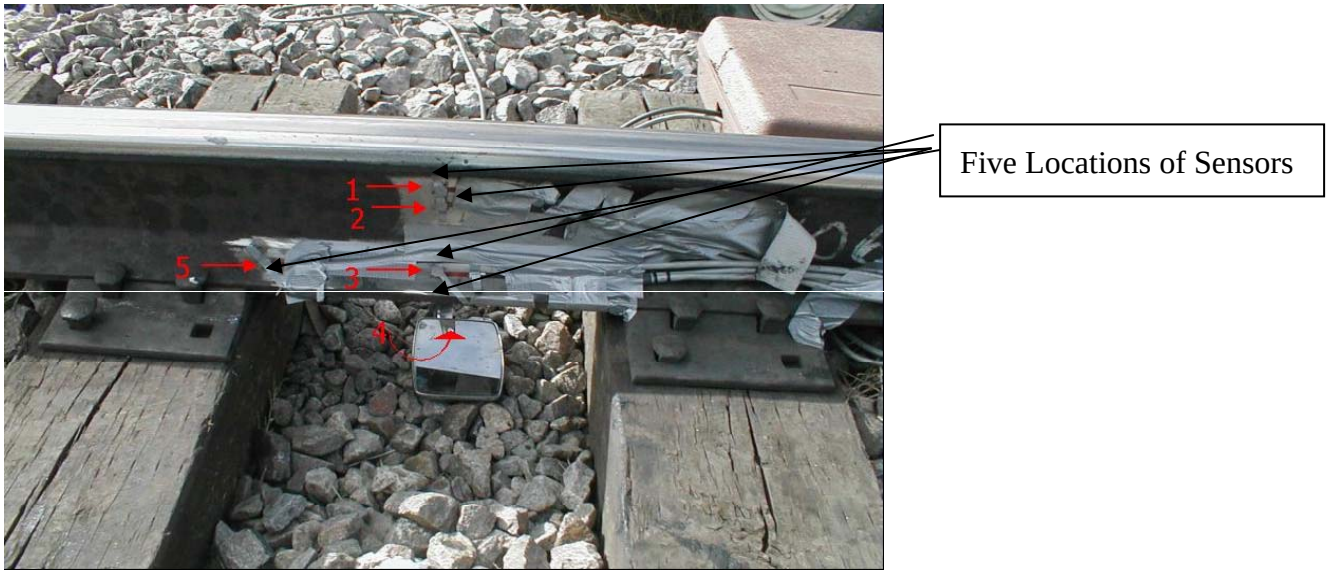

FIGURE 4-3 Five BiAST's installed at critical locations connected to PC through the cable.

4.3 STATIC LOADING TEST

As shown in Figure 4-4, the BiAST system was tested for static loading using the TTCI's Track Loading Vehicle (TLV). This TLV is built in a locomotive frame and is capable of providing a known force on the rail. Forces were manually applied vertically (up to 40 kip-force) and laterally (up to 20 kip-force) to the middle of the rail crib at 5-kip increments. Data were recorded for each load step for each of the five BiAST's.

FIGURE 4-4 BiAST Installed in the Rail under TTCI's Track Loading Vehicle.

As shown in Figure 4-5, sensors were placed at the critical locations based on the FEM model; A (SN 015), B (SN 008), C (SN 021), D (SN 012), and E (SN 001). Figure 4-6 shows a plot of 500 data points collected at a data collection frequency of 423 Hz from all five BiAST's without applying a load on the rail. As shown in Figure 4-6, there is a wide range of variations in strain measurements up to 50 micro-strains with a few spikes reading 100 micro-strains or greater. Table 4-1 summarizes means and standard deviations of five hundred data points collected from each sensor. The results vary significantly from the previous test results performed at the laboratory (See Tables 2-1 and 2-2). For example, the average microstrain value for sensor B in the Y (vertical) direction was 3.19 in the lab tests, compared with minus 0.64 in the field. This was yet another indication of stability and accuracy problems.

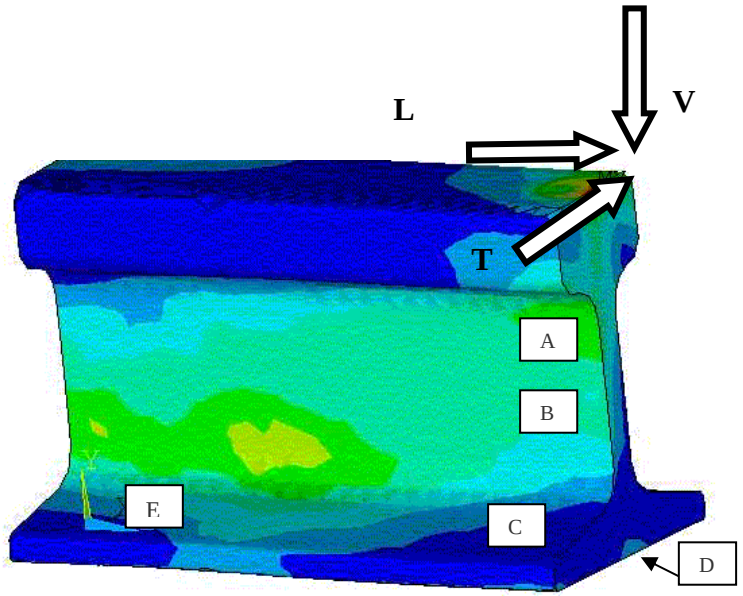

Figure 4-5. Critical locations for sensors

FIGURE 4-6 Strains measured from five sensors installed on TLV without loading.

Table 4-1. Summary of No Train Data Collected at All Five Sensors

	A: Sensor 015		B: Sensor 008		C: Sensor 021		D: Sensor 012		E: Sensor 001	
	Vert.	Long.	Vert.	Long.	Trans.	Long.	Trans.	Long.	Trans.	Long.
Avg.(microstrain)	N/A	N/A	-0.64	-7.58	28.65	7.16	3.04	2.02	18.80	-26.4
Std Dev (microstrain)	N/A	N/A	2.19	2.56	17.39	3.11	0.83	1.85	20.29	9.78

The TLV applied forces up to 40 kip-force vertically and up to 20 kip-force laterally at 5-kip increments to the middle of the rail crib. Up to 20,000 data points were recorded from the five BiAST's simultaneously at a data collection frequency of 423 Hz for each load level. Figures 4-7 to 4-11 show the strain values obtained from the five sensors A, B, C, D, and E at each vertical load level up to 40 kips at 5-kip increments. The FEM results corresponding to the same vertical loading conditions were computed and plotted along with the actual data points. In general, strain values increased as the load increased in both longitudinal and vertical directions. However, all strain values did not increase linearly as the load increased. In addition, there are substantially differences between collected data and the strain values as predicted by the FEM model. It should be noted that the sensor A worked at this time although it did not work in the earlier test. These test results also indicate that the BiAST sensor is unstable and unreliable.

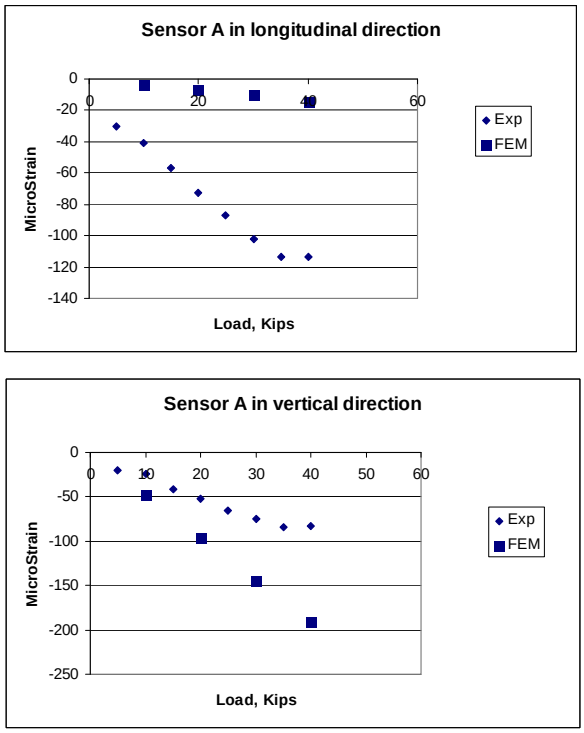

FIGURE 4-7 Vertical loading vs. corresponding strain for BiAST™ A in both directions.

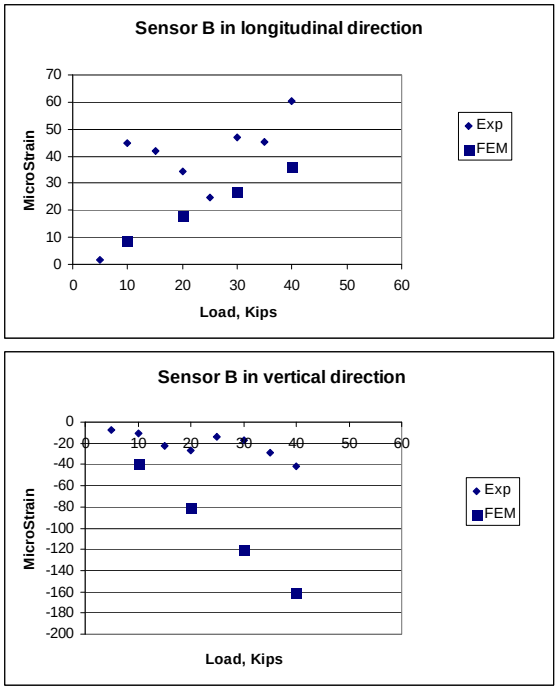

FIGURE 4-8 Vertical loading vs. corresponding strain for BiAST™ B in both directions.

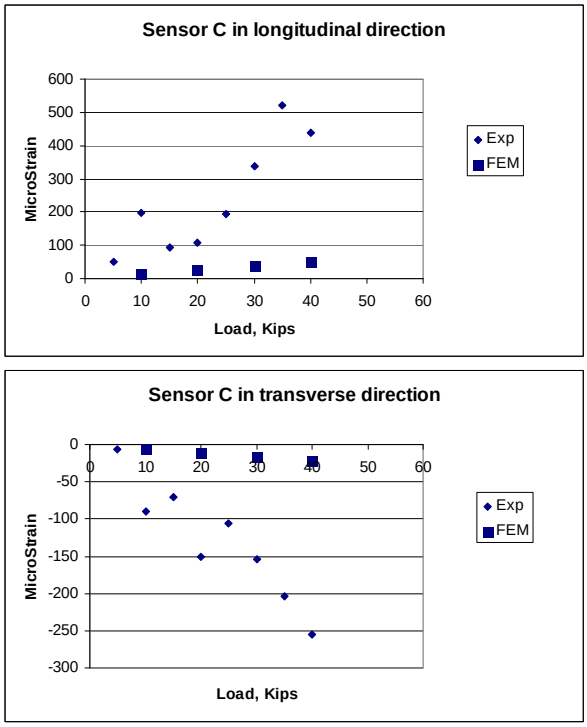

FIGURE 4-9 Vertical loading vs. corresponding strain for BiAST™ C in both directions.

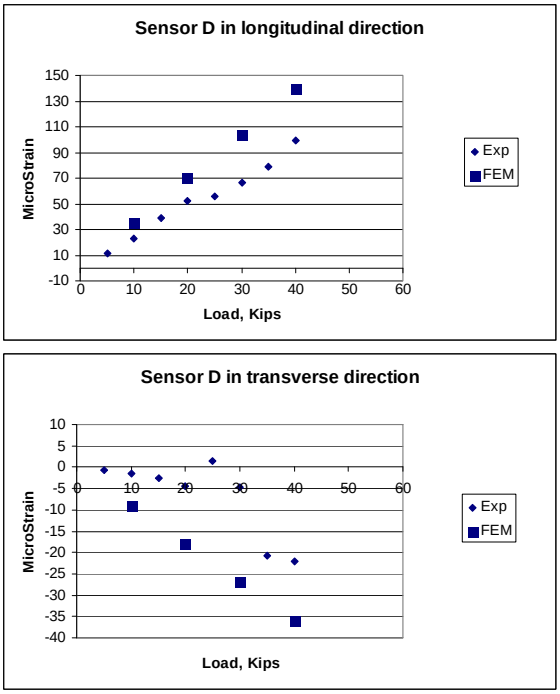

FIGURE 4-10 Vertical loading vs. corresponding strain for BiAST™ D in both directions.

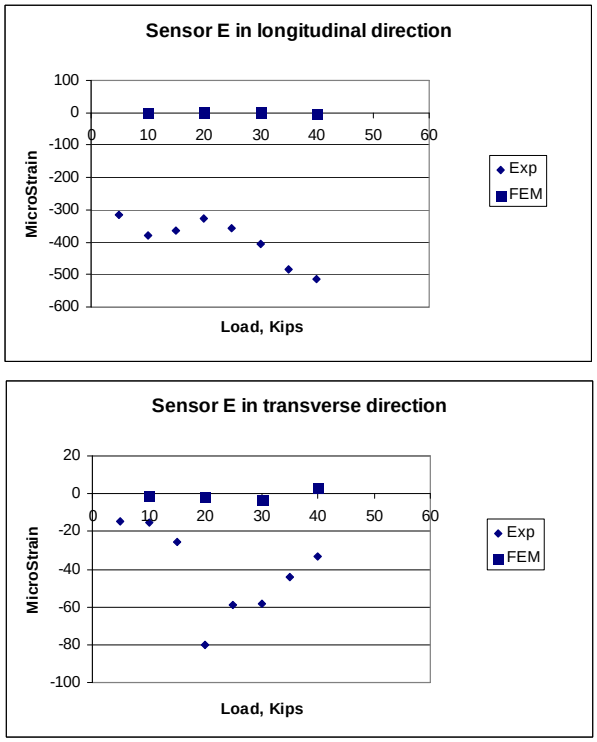

FIGURE 4-11 Vertical loading vs. corresponding strain for BiAST™ E in both directions.

These field test results under no-load conditions and under static TLV load conditions showed significant non-linearity, high noise levels, and large variations between predicted and measured strains. These results identified serious problems with the BiAST system. Possible factors contributing to these problems include problems with the installation of the sensors on the rail, and inherent stability and accuracy problems with the BiAST system.

5 DYNAMIC LOAD TESTING IN THE FIELD

Strain data were collected continuously from the real-time FAST test track from April 29 through May 2, 2002. The BiAST system was installed during the day and the strain data were collected during train operations from 10:00 p.m. to 7:30 a.m. The train was comprised of 4 locomotives and 78 cars. Most of the cars were loaded up to 315,000 lbs of total weight on 4 axles. The total train weight was approximately 12,000 tons. The train operated at speeds up to 40 mph.

5.1 REAL-TIME STRAIN DATA COLLECTION

Real-time strain data were collected continuously and saved into a laptop computer. Individual laps of train operation were extracted from the raw data to monitor the real-time strain caused by a single passage. Figure 5-1.a shows a complete set of the strain data collected using a BiAST installed at the bottom of a rail (Location D) under a train with a speed of 40 mph at a data collection frequency of 423 Hz for 75 seconds. The strain data clearly indicates the locations of peaks and valleys due to the bending and compression stresses caused by a running train. Tensile strain values were measured up to 800 micro-strains. As illustrated in Figure 5-1.b, the strain signatures from the trainload are distinctively clear, corresponding to each wheel, which can be used for a fatigue analysis of a rail.

Figures 5-2 through 5-5 show examples of strain spectrum collected for one lap of the train passing on all installed BiAST's on the tangent section at FAST. First, it should be noted that the sensor A did not work this time although it worked in the previous test. This confirmed that the BiAST sensor A was unreliable. As shown in Figure 5-2, in the longitudinal direction, BiAST B showed a strain spectrum with a very small mean, where the strain varied between 150 micro-strains in tension and –200 micro-strains in compression. In the vertical direction, BiAST B produced a high compressive mean value with strain values up to 500 micro-strains. As shown in Figure 5-3, in both the longitudinal and transverse directions, BiAST C produced inconsistent readings and the sensor C was determined to be unstable. As shown in Figure 5-4, in the longitudinal direction, BiAST D produced a realistic level of tensile strains that reached up to 1,100 micro-strains. In the transverse direction for this sensor, the strains stayed around 200 tensile and compressive micro-strains. As shown in Figure 5-5, BiAST E produced unrealistic readings in both longitudinal and transverse directions. In conclusion, only two sensors, B and D, produced reasonable strain values while three sensors, A, C, and E, did not work reliably.

As shown in Figure 5-6, to determine the repeatability of measurements from Sensor D, two sets of measurements were made from the train run at two consecutive laps, the fifth and the sixth. Two measurements were nearly identical although the measurements at the sixth lap were stretched over time, possibly due to a lower train speed at the sixth lap. The peak strain values under the first seven wheels measured at eleven consecutive laps are summarized in Table 5-1. The standard deviation of ten measurements for each wheel ranged from 26 to 97 micro-strains, which indicates a lack of stability over repeated peak strain measurements.

TABLE 5-1 Microstrain measurements from seven wheels for laps 10 through 20

Laps / wheel	10	11	12	13	14	15	16	17	18	19	20	Average	Std. Dev.
1	649	652	688	659	643	603	399	665	650	458	670	612	94
2	436	423	452	471	419	430	539	463	541	472	533	471	47
3	560	573	565	513	585	512	541	564	557	591	563	557	26
4	584	574	638	627	599	573	458	576	570	637	495	576	56
5	382	448	506	478	729	448	569	505	582	637	552	531	97
6	644	585	640	585	605	569	593	545	651	760	649	621	58
7	567	601	620	624	647	612	735	731	589	604	721	641	60

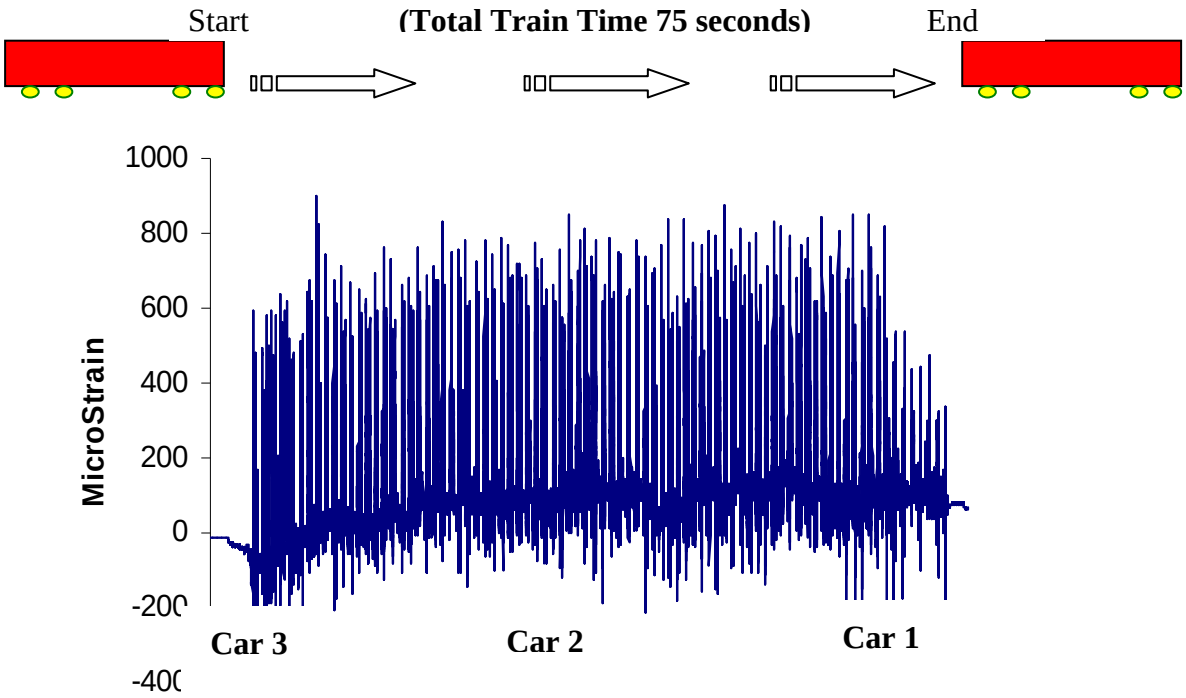

(a) Set of strain data from the bottom of rail

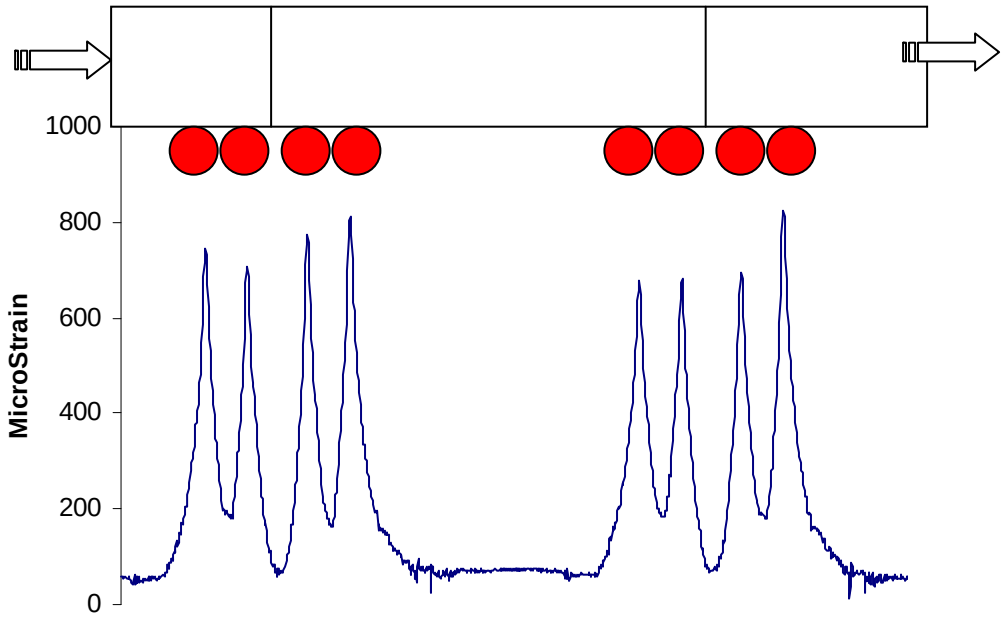

(b) Strain signatures corresponding to train wheels

FIGURE 5-1 Strains measured from sensor D under moving train loads.

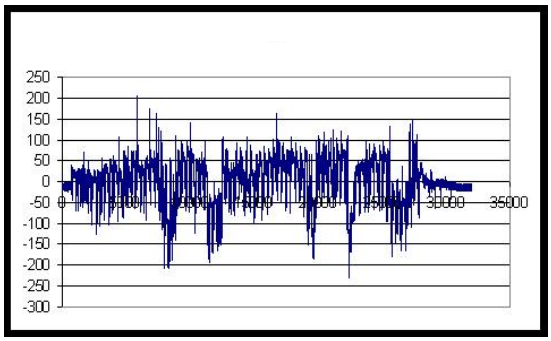

(a) Longitudinal strain of sensor B

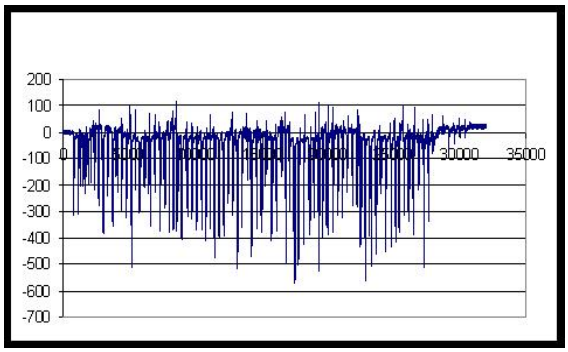

(b) Vertical strain of sensor B

FIGURE 5-2 Strain spectrums for BiAST™ B for train passing on tangent section at FAST at TTCI.

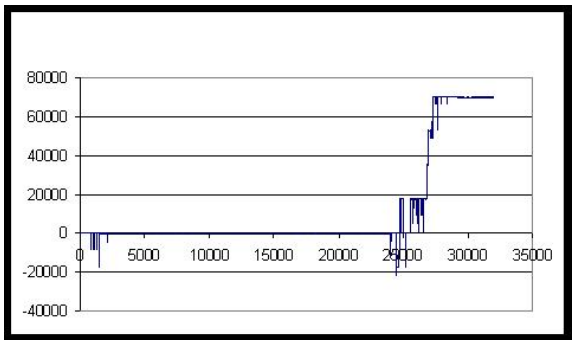

(a) Longitudinal strain of sensor C

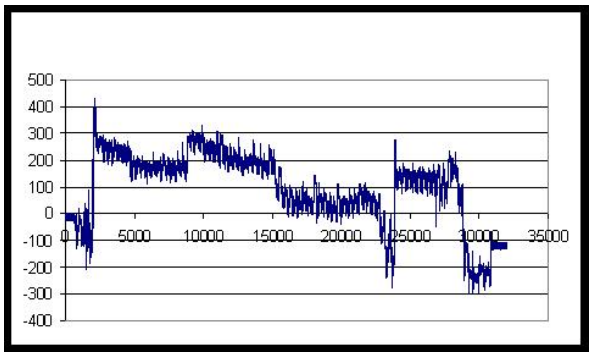

(b) Transverse strain of sensor C

FIGURE 5-3 Strain spectrums for BiAST™ C for train passing on tangent section at FAST at TTCI.

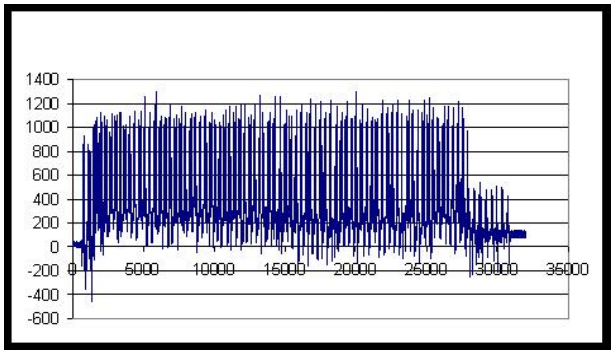

(a) Longitudinal strain of sensor D

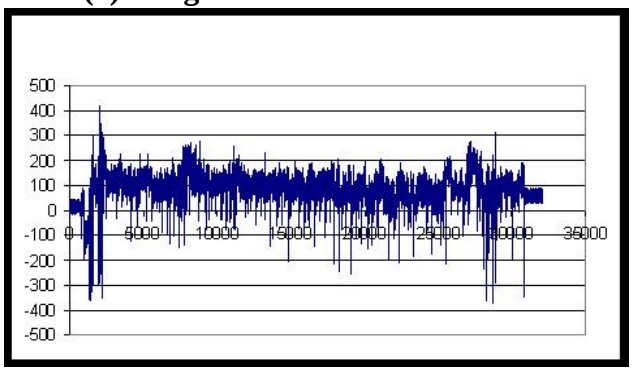

(b) Transverse strain of sensor D

FIGURE 5-4 Strain spectrums for BiAST™ D for train passing on tangent section at FAST at TTCI.

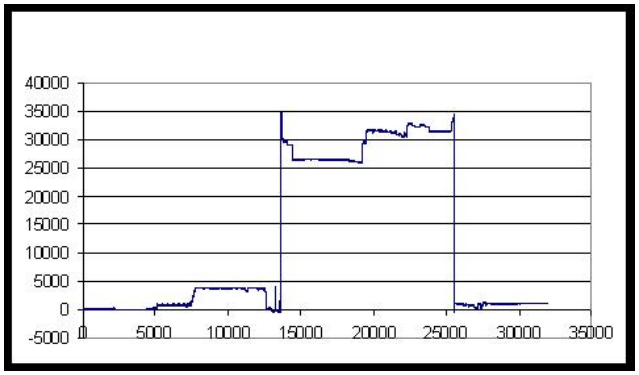

(a) Longitudinal strain of sensor E

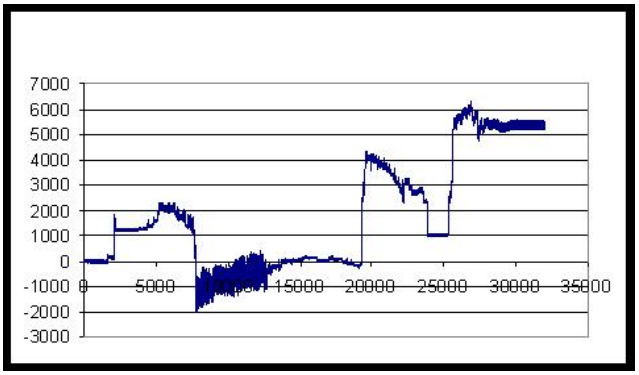

(b) Transverse strain of sensor E

FIGURE 5-5 Strain spectrums for BiAST™ E for train passing on tangent section at FAST at TTCI.

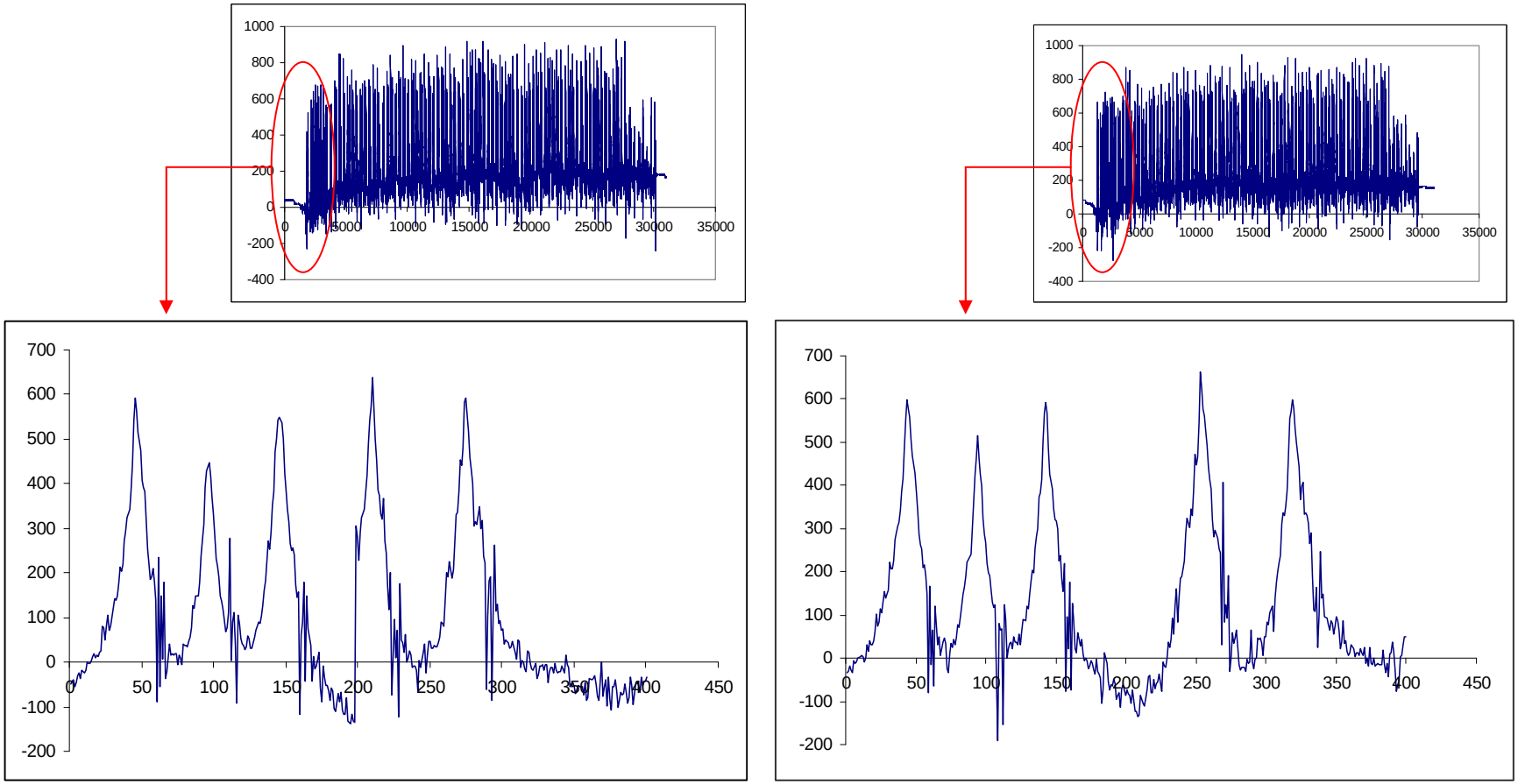

(a) Strains Measured from the first locomotive at fifth lap

(b) Strains Measured from the first locomotive at sixth lap

FIGURE 5-6 Two consecutive measurements from Sensor D mounted under the rail

Figure 5-7 shows a summary of maximum, minimum, median, and mean longitudinal strain values collected from sensor D for 21 consecutive train passages. Maximum tensile strain was found to be consistently in the range between 850 and 950 micro-strains. Maximum compressive strains were consistently measured around –300 microstrain for all laps. Mean strain measured by the BiAST sensor D was around 200 microstrains for all measured train laps. The strain measurements of this BiAST sensor show significant variations for all train laps over the instrumented section.

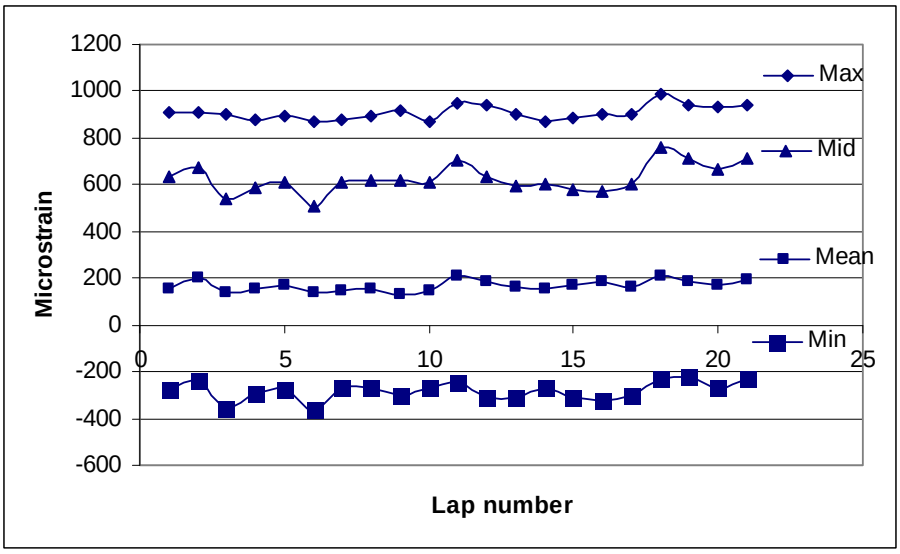

FIGURE 5-7 Repeatability of strain values at different laps of the train.

5.2 STRAIN MESUREMENTS OF ALL TRAIN LAPS

As shown in Figure 5-8, the averages of peak longitudinal strain values collected from the BiAST sensor D are plotted up to 60 laps. Each data point represents an average strain value for the test train with 320 wheels. The sensor D collected a total of 22,400 load cycles, where recorded strain values increased steadily over time. The increase could have been caused by residual strain development in the BiAST sensor itself and/or a cumulative strain buildup in the rail due to a gradual increase in rail temperature with accumulating laps, perhaps as a result of rail creep in the instrumented rail section. As noted in Figure 5-8, the rail temperature steadily increased over 60 laps. The increased temperature could have affected the stability of the BiAST sensor. The temperature sensitivity of BiAST sensors was not investigated in this study. Any further investigation and development of BiAST sensors for such applications should include the effects of temperature.

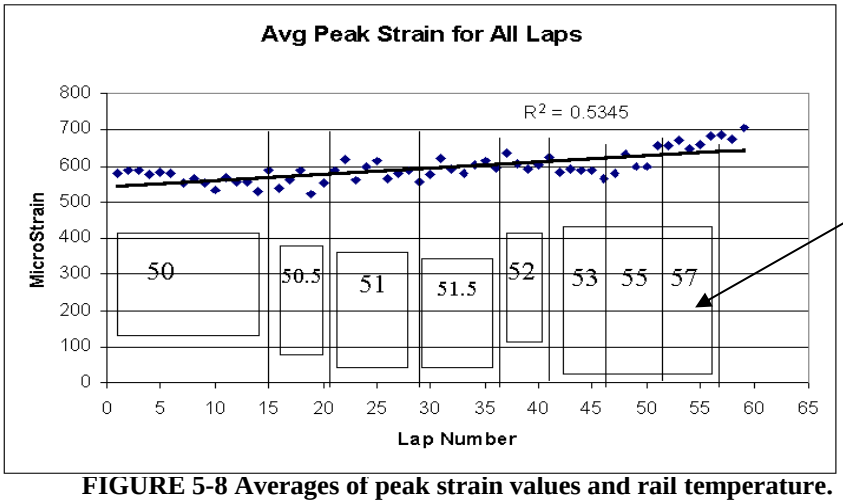

FIGURE 5-8 Averages of peak strain values and rail temperature.

6 FATIGUE LIFE PREDICTION

The strain data obtained from the BiASTs at different locations represent sets of train strain spectrum associated with each lap. Each strain spectrum for each lap can be used as an input for a rail fatigue model, provided the necessary rail material properties are known. The Rainflow cycle counting method can be utilized to count the number of cycles at various strain ranges and mean strain combinations. The number of cycles to failure can be calculated using Morrow's S-N fatigue life model (20). The average S-N curve is useful for comparing test results from different laboratories but does not represent typical service usage of rails, for which wear generally limits the useful life up to approximately 1,000 MGT. This is a relatively short life in comparison with the average fatigue life of rail steel. Therefore, the first percentile S-N curve, a time at which one percent of a large sample of specimens to form a crack, is often used to model rail fatigue life. Fatigue damage can then be computed for each strain level and mean stress using the Palmgren-Miner model (21).

This fatigue analysis procedure was implemented in the software package called "Binner," which uses the strain-life approach for estimating fatigue life using the strain spectrum from the BiAST system. The Binner finds peaks and valleys from strain spectrum, count the load cycles, and identify the maximum and minimum values for a given filter value. It is very important to remove the small ripples of cycles because they have a minimal effect on fatigue life estimation and significantly increase memory requirements.

The input of the software requires one-column or multi-column data in a text format. The input includes a sequence of peaks and valleys of the train strain spectrum over time for each lap. To minimize the on-chip data storage requirements, it is necessary to eliminate any temporal ordering of the filtered peak and valley data points. The filtered data can be stored in a user-definable two-dimensional array by computing the mean and amplitude of each valley-to-peak and peak-to-valley transition. As a result, each bin in the two-dimensional array would contain the number of half-cycles of strain counted within the bin's boundary limits for cycle means and amplitudes.

For example, the cycle counting method would produce a histogram of amplitude and mean strain values as shown in Figure 6-1. This histogram represents the number of cycles that occur in the strain history at specific amplitudes and mean strains. The strain amplitude axis is divided into 10 ranges from 100 micro-strains to 1,188 micro-strains and the mean strain axis is divided into 10 ranges from –175 micro-strains to 812 micro-strains. The input file can have up to 40,000 rows of strain data and the output file contains peaks, valleys, and number of cycles. Number of cycles to failure is then computed for each combination of amplitude and mean strains.

The BiAST system can be a great tool for detecting the dynamic response of any particular wheel in the train and for documenting spurious overload events. This capability can provide valuable information on passing wheels, such as vehicle speeds, track conditions, and vehicle conditions such as flat wheels. If the remaining life is predicted based only on the strain history to date, however, the actual remaining life could be less than predicted due to such factors as the deterioration of the overall track structure over time, e.g., deterioration of ballast or sub-grade conditions.

The original work plan for this project called for the development of estimates of remaining fatigue life using the fatigue life model developed in this project and the BiAST data collected in the field. It became obvious, however, that the poor quality of the test data would not enable such an application.

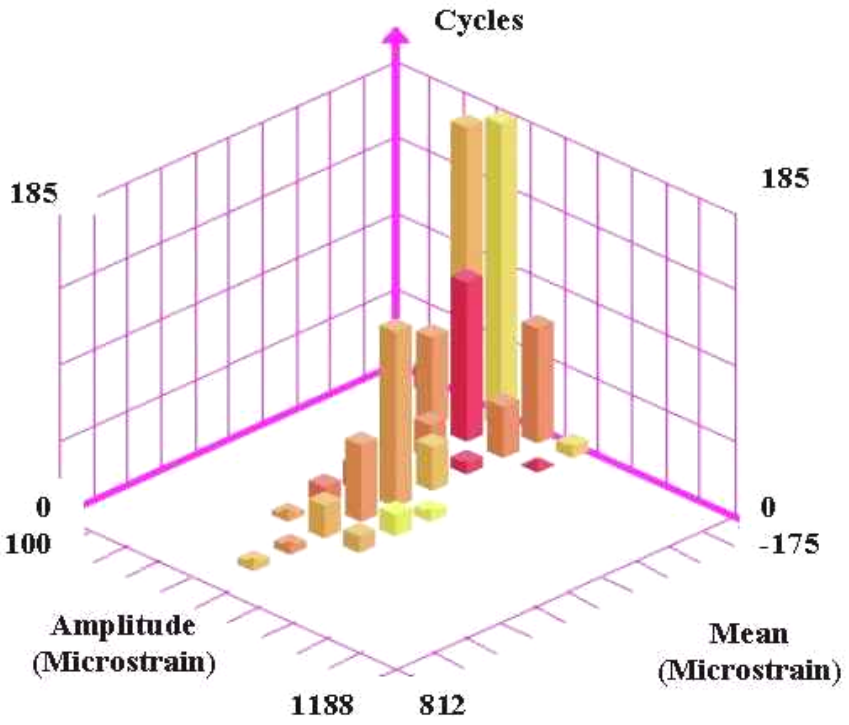

FIGURE 6-1 Sample histogram of amplitude and mean strain values caused by a train.

7 FABRICATION OF A PROTOTYPE HYBRID BIAST SYSTEM

Findings from the preliminary BiAST testing at TTCI indicated substantial improvements are required in order to develop a commercial-grade system. Steps required include the following:

- Develop improved procedures to more easily and reliably attach the BiAST sensors to the rail.
- Determine the causes for the lack of stability, accuracy, and high noise levels of the sensors, and whether these problems can be corrected.
- If these problems can be satisfactorily resolved, the next step would be to incorporate the BiAST sensors into a hybrid system that would include a peripheral interface controller (PIC) with on-chip data storage and data processing.
- The final step would be to return to TTCI with the improved system for a second series of field tests, followed by the analysis of the test data.

The subcontractor that developed the BiAST sensors was expected to develop a hybrid system capable of processing the strain data. Unfortunately, the subcontractor was unable to develop the hybrid system. The University of Iowa team attempted to develop a hybrid system, including a circuit board for a commercially-available PIC, power supply circuits, and PIC layout and connections. However, we were unable to obtain the specific protocol to enable the BiAST sensors to communicate with the PIC. As a result, none of the steps outlined above were performed, and plans for a second field test had to be abandoned.

Our final effort involved simulating the data coming from the BiAST and processing it using a new controller box using PIC 16F877. It was assumed that the data is already obtained from the BiAST sensor and ready to be processed by the PIC microcontroller. As shown in Figure 7.1, we created a new circuit board for PIC16F877 which is designed to include two main parts (1) EEPROM: “Electronically erased programmable read only memory” chip to store data and (2) serial port to enable communication between PIC16F877 and the PC for downloading data stored in the EEPROM. The remaining parts of the circuit include a clock, switch button, capacitors and transistors and all necessary connections to complete the circuit. PIC16F877 is connected to all necessary parts and works as the manager of the circuit board.

As shown in Figure 7-2, a small program was developed to enable PIC16F877 to write and read data using EEPROM, counting and categorization of the number of the peaks in the cycles and, transfer the results to a PC. The sample code was written in a C language environment specially designed for PIC programming. Using the PICSTART plus development tool as shown in Figure 7-3, the C language code was compiled into a final “.hex” format file that can be downloaded into the PIC16F877. MPLAB software was then used to download the code into the PIC. Since our program has been already compiled using the C compiler, it was not necessary to rewrite the code in assembly language using MPLAB software.

Seven steps involved in the development and programming of PIC16F877 are depicted in Figure 7-4 and each step is briefly summarized below.

1. Design the circuit board for communication and basic functions.
2. Develop a program for storage and manipulation of data.
3. Compile the C program into a “.hex” format using PICSTART plus development programmer.
4. Download the program in “.hex” format into the PIC using MPLAB IDE software.
5. Place the programmed PIC into the designed circuit board.
6. Establish a communication between circuit board and PC.
7. Download the processed data into PC for further analysis.

Figure 7-1. Picture of PIC16F877 circuit board.

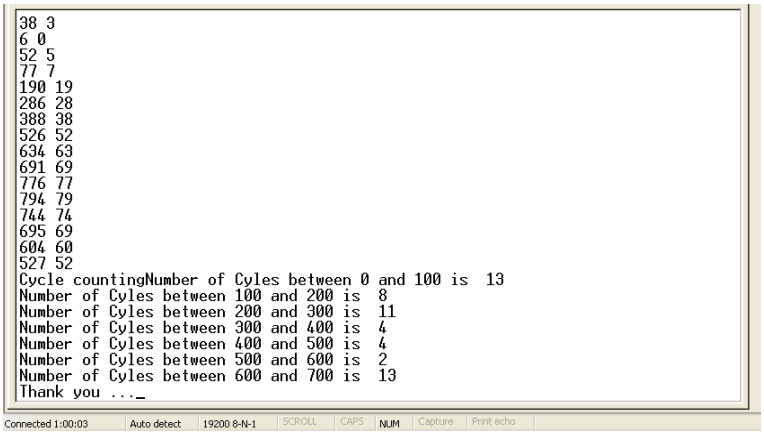

Figure 7-2. Display of raw strain data and their categorization.

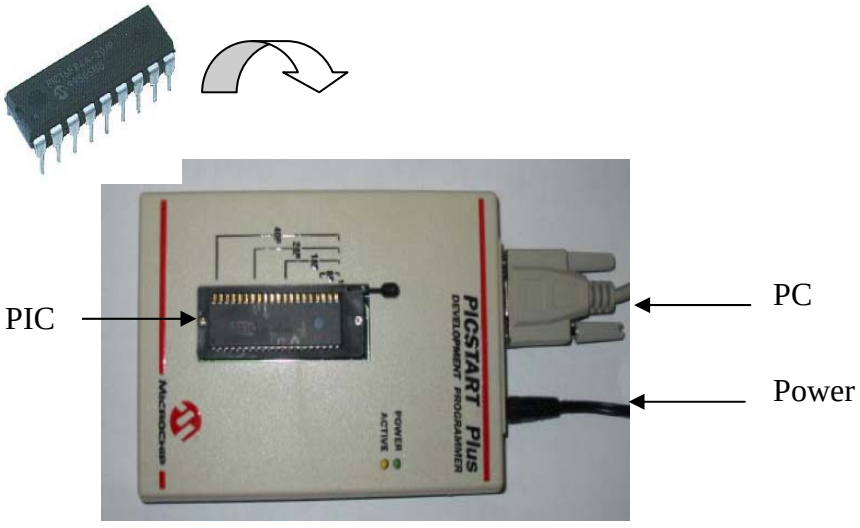

Figure 7-3. PICSTART plus development programmer.

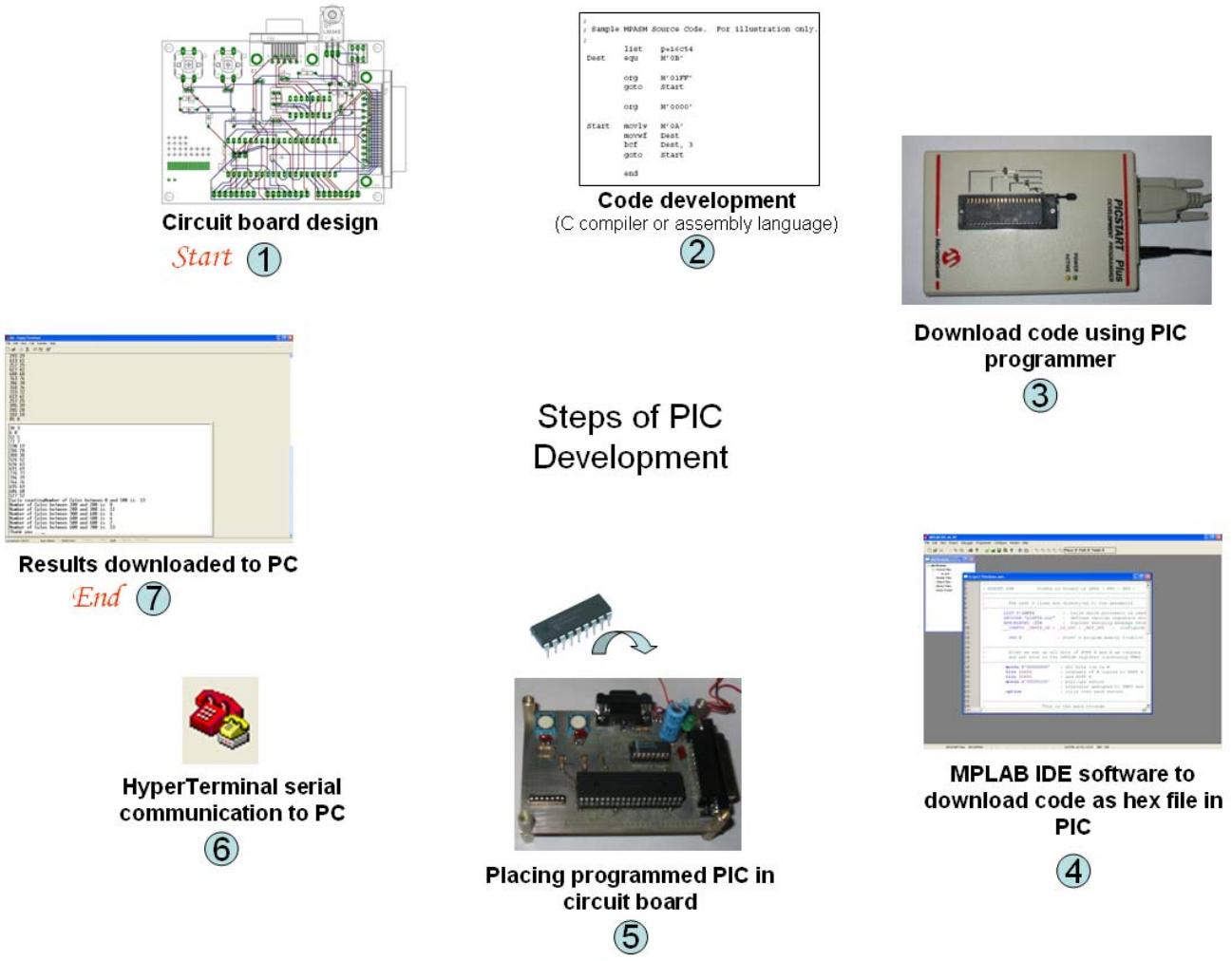

Figure 7-4. Seven Steps involved in the development of PIC16F877.

8 CONCLUSIONS AND RECOMMENDATIONS

8.1 SUMMARY OF TASKS

The objective of this research was to develop a prototype hybrid BiAXIAL Strain Transducer (BiAST) sensor to predict rail fatigue life based on strain history. Due to serious issues with bonding of the earlier prototype UASTs to rail, much emphasis was placed on finding a more effective method for attaching and detaching the transducers to the rail. To this end, an approach was developed where mounting "stems" are first bonded to the test surface and proof-loaded. The BiAST device is then placed over the mounting stems and secured using small clevises and tightening screws. Moreover, replacing a given device is simplified since no surface preparation and rebonding of attachment feet is necessary; one simply loosens and replaces the old device with a new one (12). Field application of the BiAST sensors using this method revealed that it is very difficult to install the mounting stems on the rail, so additional refinements are needed.

To identify the critical locations where these BiAST sensors are to be installed, a three-dimensional finite element model (FEM) of the rail structure was developed with all necessary boundary conditions and loading configurations. The FEM analysis identified five locations that would experience the highest stresses resulting from the loading configuration of a train. Using the data acquisition software, strain data was collected using five BiAST sensors for three different types of loading: no loading, static loading, and dynamic loading. The "no loading" condition was used to determine the noise level in the BiAST sensors. During the "no loading" testing process, only two of the five BiAST's consistently indicated unbiased zero noise. One BiAST unit located near the rail head showed no response, although its wiring and setting were all properly configured. The Y-axis in two other BiAST sensors produced a significant amount of bias between –60 microstrains in compression and +90 microstrains in tension. The BiAST system was then tested for static loading using the Track Loading Vehicle (TLV) at TTCI near Pueblo, Colorado. Both vertical and lateral loading conditions were studied on the rail section under testing. In general, BiAST sensors produced the increased strain as the load increased. However, most BiAST's failed to produce consistent linearity of strain with increased load, as predicted by the FEM model.

The five BiAST sensors were installed on a rail to collect real-time strain data from the Facility for Accelerated Service Testing (FAST) at TTCI. BiAST devices were tested under a real-time heavy axle loading condition of a 78-car train. Strain data were collected continuously but only two out of the five BiAST sensors produced reasonable strain values. One BiAST sensor installed at the bottom of the rail (the underside of the web) measured a tensile strain up to 800 micro-strains in the longitudinal direction of a rail. This result was verified by the FEM model, which produced a strain value up to 680 micro-strains for the same condition. The maximum tensile strains were measured from this BiAST sensor installed under the rail in the longitudinal direction and they consistently ranged between 850 and 950 micro-strains. Maximum compressive strains were measured at around –300 micro-strains for all laps of the train.

The fatigue analysis procedure was implemented in software called "Binner," which is designed for integration into the programmable chip of the BiAST to monitor rail structures at remote locations. The objective was to analyze the BiAST data collected in the field using the "Binner" fatigue analysis program for counting the load cycles and estimating the fatigue life of a rail structure. The Binner finds peaks and valleys from strain spectrum, count the load cycles, and identify the maximum and minimum values for a given filter value. It is very important to remove the small ripples of cycles because they would have a minimal effect on fatigue life estimation, and significantly increase memory requirements. A sensitivity analysis was performed on the strain spectrum to determine the effect of eliminating small ripples of cycles on the fatigue life estimation. Reasonable estimates of fatigue life using the BiAST data could not be developed, however, due to the data quality problems described previously.

8.2 CONCLUSIONS AND FINDINGS

The field evaluation of the BiAST system at TTCI determined that several problems will need to be resolved prior to implementing this technology. It is very difficult to install the mounting stems for the BiAST sensors on the rail in the field. After installation, three of the five sensors didn't work at all, and the other two performed inconsistently. The current BiAST system lacked repeatability and accuracy. Attempts to incorporate a fatigue analysis module in the sensor system were unsuccessful. Any further development of this technology for such rail applications will require investigation of the causes of, and solutions to, the problems identified in this project. Our conclusions and recommendations are summarized below.

1. Based on our field evaluation, the current BiAST sensors should be considered unstable. Only two out of five sensors produced reasonable measurements and the other three sensors produced inconsistent strain values.
2. Field test result indicates a significant variation among repeated peak strain measurements under each train wheel.
3. A major limitation is the difficulty of attaching very small mounting stems on a rail and attaching BiAST sensors to the stems using tiny screws. There is a potential for error in accurately locating small stems with the proper orientation.
4. A three-dimensional finite element model for rail has been developed to compute stresses under train wheel loads and to identify critical strain locations for the installation of BiAST sensors.
5. Software was developed to predict fatigue life using the Rain-flow cycle counting algorithm, and based on a strain-life model and cumulative damage concept.
6. A prototype BiAST system was fabricated to demonstrate a concept that can integrate "Binner" software on the programmable chip of the BiAST to monitor rail structures at remote locations.
7. The BiAST can be considered as a potential tool for detecting the dynamic response of a train and for documenting spurious overload events. This capability of the BiAST could provide valuable information from passing trains such as speed, track conditions, and rolling stock condition.

Since the actuation wires and bellows of BiAST sensors are compliant in bending in order to facilitate changes in substrate curvature, the BiAST package effectively sits on a bed of springs. The instability of the BiAST sensors we experienced could have been caused by a dynamic excitation of the rail caused by a train which could cause unwanted motions and create errors in the strain measurements. The following aspects of BiAST sensors should be corrected in the future: 1) fix the token-passing communication interface, 2) fix the temperature sensor interface, and 3) redesign the detector output buffer amplifier to provide more headroom and make the number of strobes less critical for good noise and linearity performance (12).

Recently, Sarcos Research Corporation fabricated over 600 UAST-based single-axle load cells for a railcar load monitoring application (12). In the future, we recommend a significant effort be made on improving the field installation procedures for BiAST sensors and enhancing their stability and accuracy. In addition, to be operated by battery power in the field, an auto-wake/sleep mode of operation will be required to reduce power during periods of low strain activity. A micro-power RAM could be employed to preserve the contents of load cycle counting registers during sleep mode. Data from these registers should be recovered periodically in order to predict the remaining fatigue life and identify spurious overload events in a rail structure.

REFERENCES

1. O. Orringer and J. M. Morris. *Applied Research on Rail Fatigue and Fracture Mechanics in the United States.* Theoretical and Applied Fracture Mechanics, Vol. 1, 1984, pp. 23-49.
2. T. Baldwin and E. Mech. *Significance of the Fatigue of Metals to Railways.* Proceedings of the international conference on fatigue of metals, New York, 1956
3. J. W. Ringsberg. *Life prediction of rolling contact fatigue crack initiation.* International Journal of Fatigue", Vol. 23, 2001, pp. 575-586.
4. D. F. Cannon and H. Pradier. *Rail rolling contact fatigue*, Research by the European rail research institute, Wear, Vol. 191, 1996, pp.1-13.
5. R.I. Stephens, A. Fatemi, R.R. Stephens, and H.O. Fuches. *Metal Fatigue in Engineering*. Second edition, Wiley, 2000.
6. R. C. Rice and D. Broek. *Fatigue Crack Initiation Properties of Rail Steels*. Report DOT/FRA/ORD-82/05, final report to the U.S. Department of Transportation, Federal Railroad Administration, Washington, D. C., 1982.
7. F. K. Dunker and G. B. Rabbat. *Assessing infrastructure deficiencies: The case of highway bridges.* ASCE Journal of Infrastructure Systems, June, Vol. 1 No. 2, 1995, pp. 100-119.
8. W. J. McCarter, R. M. Chrisp, A. Butler, and P. Basheer. *New surface sensors for condition monitoring.* Construction and Building Materials 15, 2001, pp. 115-124.
9. Neubert and K.P. Hermann. *Instrument Transducers - An Introduction to their Performance and Design*, 2nd Edition, Oxford University Press, London, 1975.
10. S. Middelhoer and A. C. Hoogerwerf. *"Smart sensors when and where", Sensors and Actuators* 8, 1985, pp. 39-48.
11. B. J. Maclean, M. G. Miladejovsky, M. R. Whitaker, and M. Oliver. *A digital MEMS-based strain gage for structural health monitoring*. Proceedings of MRS Conference, Boston, 1997
12. DABT-63-98-C-0048, 2002. *Low Profile, Low Power Uni- and Multi-Axial Strain Transducers (LP2-UAST/MAST)*, Final Report, Sarcos Research Corporation, Salt Lake City.
13. H. Lee, H. Yun, and B. Maclean *Development and field testing of a prototype hybrid uniaxial strain transducer*, NDT & E international, 2001.
14. O. Zienkiewicz and R.L. Taylor. *The Finite Element Method*, 5th ed. Oxford, Boston, Butterworth-Heinemann, 2000.
15. V. A. Profillidis. *Railway Engineering*, Second Edition, Asghate Publishing Limited.
16. J. J. Scutti, R. M. Pelloux and R. Fuquen-Moleno. *Fatigue Behavior of a Rail Steel, Fatigue Engineering Materials*, Vol. 7, No. 2, pp. 121-135, 1984.
17. A. M. Zaremski. *Effect of Rail Section and Traffic on Rail Fatigue Life*, American Railway Engineering Association Bulletin, 673, Vol. 80, pp. 514-527.
18. O. Orringer. Control of Rail Integrity by Self-Adaptive Scheduling of Rail Tests, FRA, U.S. DOT, DOT/FRA/ORD-90/05, 1990.
19. J. Sun. Bending Fatigue Properties of Rail Welds. Technical Digest, 02-026, TTCI, November 2002.
20. J. W. Ringsberg and M. Loo-Morrey, B.L. Josefson, A. Kapoor and J.H. Beynon. *Prediction of fatigue crack initiation for rolling contact fatigue* International Journal of Fatigue, 22, 2000, pp. 205-215.
21. M. A. Miner. *Cumulative damage in fatigue*, Trans. ASME, J. Appl. Mech., Vol. 67, Sept., 1945, PA 159.